PNAS RESEARCH ARTICLE | ENGINEERING NEUROSCIENCE

Neurochemical imaging reveals changes in dopamine dynamics with photoperiod in a seasonally social vole species

Jaewan Mun[a,1], Kelley C. Power[b,1], Natsumi Komatsu[a,c], Sophia A. Tomatz[d], Annaliese K. Beery[b,e,f,2], and Markita P. Landry[a,e,f,g,2]

Affiliations are included on p. 10.

Edited by Catherine Murphy, University of Illinois at Urbana-Champaign, Urbana, IL; received April 18, 2025; accepted December 2, 2025

Studying dopamine signaling in nonmodel organisms is crucial for understanding the broad range of behaviors not represented in traditional model systems. However, exploring new species is often hindered by a scarcity of tools suitable for nongenetic models. In this work, we introduce near-infrared catecholamine nanosensors (nIRCats) to investigate dopamine dynamics in meadow voles, a rodent species that exhibits distinct changes in social behavior and neurobiology across photoperiods. We observe increased dopamine release and release site density in voles housed in short photoperiods (which induce a social phenotype), suggesting adaptations linked to environmental changes. Moreover, pharmacological and extracellular manipulations demonstrate that short photoperiod/social voles exhibit heightened responsiveness to dopamine-increasing interventions and resilience against suppressive conditions. These findings highlight a significant association between dopamine signaling and photoperiod-driven changes in social behavior and establish nIRCats as an effective tool for expanding our understanding of dopamine dynamics across nonmodel organisms.

dopamine | nanosensors | photoperiod | voles | neurochemical imaging

Significance

Most neurobiological insights come from traditional model organisms, which often lack the behavioral diversity found in nature. Meadow voles, in contrast, undergo seasonal shifts in social behavior that offer a rare opportunity to study neurochemical adaptations to environmental cues. Here, we apply synthetic, near-infrared catecholamine sensors (nIRCats) to image dopamine release with synaptic resolution in this nonmodel species. We show that dopamine dynamics vary with photoperiod, with social voles in short photoperiods exhibiting greater dopamine release, heightened sensitivity to dopamine-enhancing interventions, and reduced suppression under inhibitory conditions. This work links environmental cues to synaptic dopamine signaling and highlights nIRCats as a broadly applicable tool for neuromodulation research beyond genetically tractable models.

Significant breakthroughs in neuroscience have emerged from the study of diverse species from the barn owl to the sea slug, reinforcing August Krogh's famous declaration: "for many problems there is an animal on which it can be most conveniently studied" (1, 2). Studies of diverse organisms also enable comparisons across species, improving our understanding of shared mechanisms and of species-specific adaptations (3–6). Nowhere is this more evident than in the study of social behavior, which can be highly variable between even closely related species (7–9). Although the study of diverse species is crucial, it is accompanied by methodological challenges, as many tools and techniques available in model organisms are genetically based and challenging to apply outside of the model organisms for which they have been developed. The development of nongenetically encoded neurochemical sensors that can be applied in wide-ranging species promises to advance research on behaviors exhibited only by "weird," nontraditional species. Here, we validate and apply synthetic catecholamine sensors to investigate photoperiod-driven changes in dopamine release, reuptake, and diffusion in the striatum of meadow voles (*Microtus pennsylvanicus*), a nonmodel organism that offers a rare opportunity to study pathways underlying seasonal changes in social dynamics. Using our tool, we find previously uncharacterized dopamine signaling differences in voles under short photoperiods in which they exhibit increased social interactions, indicating a potential role for changing dopamine in mediating this shift.

Dopamine, a neuromodulatory catecholamine most often associated with reward and pleasure, also plays important roles in regulating social behavior. Striatal dopamine in particular is elevated after mating, facilitates social bonding following mating in some species, and is involved in social reward processing in a number of species, including humans (10, 11). However, dopamine release and modulatory dynamics at the synaptic level that may support alterations in social behaviors remain largely unknown. Many current methods used to examine dopamine dynamics are limited by spatial and/or temporal resolution. Microdialysis, although capable of measuring extracellular dopamine with high specificity, has poor spatial and temporal resolution. Fast-scan cyclic voltammetry, while able to quantify extracellular dopamine at high temporal resolution, is not capable of visualizing dopamine in high spatial resolution. Genetically encoded dopamine-based sensors have overcome many of these challenges and are capable of imaging at high temporal resolution but are often limited to use in model organisms such as mice and rats and have yet to achieve spatial resolutions enabling single release site quantification. We recently developed near-infrared catecholamine nanosensors (nIRCats) that are capable of imaging dopamine with high spatiotemporal resolution (12, 13).

This article is a PNAS Direct Submission.

[1]J.M. and K.C.P. contributed equally to this work.

[2]To whom correspondence may be addressed. Email: abeery@berkeley.edu or landry@berkeley.edu.

This article contains supporting information online at https://www.pnas.org/lookup/suppl/doi:10.1073/pnas.2509561123/-/DCSupplemental.

Published January 23, 2026.

nIRCats enable direct visualization of dopamine volume transmission by labeling the brain's extracellular space with release site resolution, and because of their synthetic nature, they can be readily used in diverse, nonmodel organisms.

Meadow voles provide a unique opportunity to study mechanisms supporting social behavior because they exhibit predictable transitions in grouping behavior within a single species in response to environmental cues (14). Meadow voles are seasonally social: Females are solitary and territorial in summer months but come together in mixed-sex groups in the winter (15, 16). In the wild, photoperiod is the primary cue many mammals use to determine the season (17, 18) and is sufficient in lab settings to induce changes in behavioral and physiological phenotypes associated with each season, including social behaviors (Fig. 1*A*). In long photoperiods (LP; 14 h light:10 h dark), female meadow voles interact less with and are less affiliative toward conspecifics than their counterparts housed in social, short photoperiods (SP; 10 h light:14 h dark). In contrast, short photoperiod voles form selective partner preferences for peer companions, and prefer to cohabit in groups (19, 20). Many neurobiological pathways change in concert with the transition between photoperiods and social phenotypes, including changes in multiple neuropeptide signaling pathways (21–23). In prairie voles, a closely related monogamous vole species, dopamine signaling is integral to the formation and maintenance of social bonds with mate partners (24–28). Photoperiodic changes in dopamine signaling have been documented in mice and chipmunks (29–31) and may contribute to changes in behavior. In meadow voles, changes in dopamine signaling across photoperiods associated with different grouping behavior have never been examined.

In the present study, we validated the use of nIRCats in meadow voles to investigate whether striatal dopamine release dynamics differed between voles housed in conditions that promote social and nonsocial behavioral phenotypes. We found that in short photoperiods, voles exhibited greater dopamine release than long photoperiod voles, both across matched and photoperiod-typical housing. We also investigated the effects of sex and regional variability within the striatum on dopamine dynamics. Finally, we modulated dopaminergic signaling using sulpiride (D2 receptor antagonist), quinpirole (D2 receptor agonist), and extracellular Ca^{2+} to explore how voles with different social phenotypes respond differently to these key regulators of dopamine signaling. In socially housed, short photoperiod voles, dopamine release was more strongly enhanced in response to dopamine-increasing manipulations. In contrast, in nonsocial, long photoperiod voles, dopamine release was more strongly suppressed in response to dopamine-decreasing manipulations. These data provide evidence for increased striatal dopamine in short photoperiods versus long, nonsocial photoperiods and establish nIRCats as a valuable tool to measure dopamine dynamics at the synaptic level in nonmodel organisms.

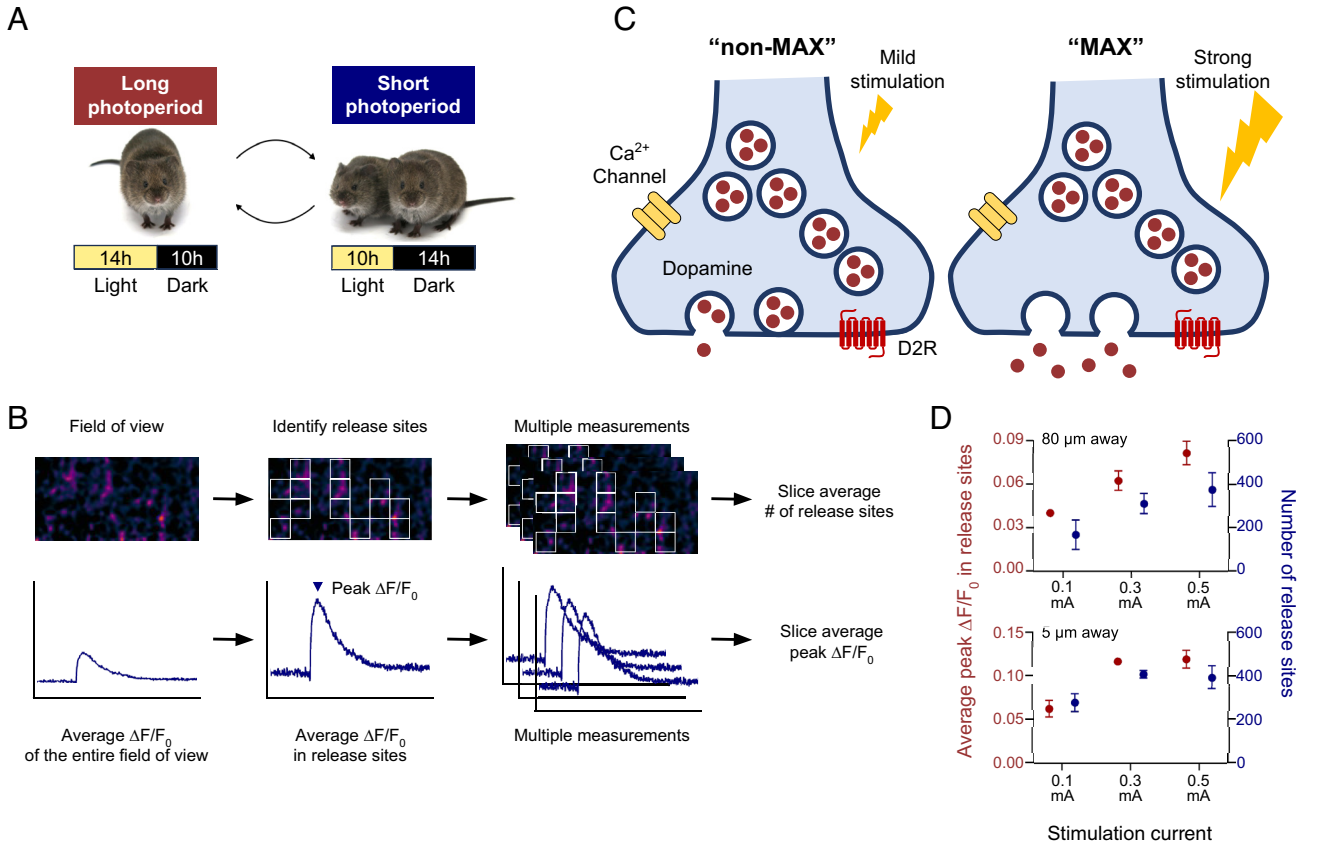

Fig. 1. Schematic of experimental design. (*A*) In lab settings, altering photoperiod is sufficient to induce changes in behavior and physiology in meadow voles, with long photoperiods associated with solitary living and short photoperiods associated with group formation. (*B*) Schematic of data analysis methods used to examine the average number of release sites and the average peak $\Delta F/F_0$ per release site in a brain slice. The number of release sites and the peak $\Delta F/F_0$ correlate with the putative number of dopamine-releasing synaptic sites and the amount of dopamine released from each site, respectively. (*C*) Schematic of dopaminergic neurons under mild (*Left*, "non-MAX") and strong (*Right*, "MAX") electrical stimulation. More dopamine is released from the readily releasable dopamine pool with stronger electrical stimulation. (*D*) Change in average peak $\Delta F/F_0$ (red, *Left y*-axis) and the number of release sites (blue, *Right y*-axis) as a function of current, with the stimulator positioned at 80 µm (*Top*) and 5 µm (*Bottom*) from the field of view. (n = 3 measurements) Stimulation with 0.3 µA/80 µm was designated as the non-Max condition, while stimulation with 0.5 µA/5 µm was designated as the MAX condition.

Results

We sought to understand how dopamine signaling might be affected by photoperiodic changes in meadow voles, as day length is the primary cue regulating a major transition in their social behavior. To investigate how photoperiod impacts dopamine signaling, we synthesized dopamine-sensitive optical probes, nIRCats, following established protocols, and used these probes to label the extracellular space of brain slices prepared from adult voles exposed to the above-mentioned photoperiods with custom near-infrared microscopy (12, 13). We hypothesized that nIRCats would enable us to image changes in dopamine signaling through the brain extracellular space induced by different photoperiod exposures. We further hypothesized that there may be subtle changes in dopamine signaling, depending on whether neuronal synapses are stimulated with a mild stimulus to release predominately their readily releasable pool of dopamine, or whether synapses are promoted to release intracellular dopamine reserves with a strong stimulus to release most intracellular dopamine.

One key advantage of nIRCats is the ability to image dopamine release and reuptake with high spatiotemporal resolution. Labeled brain slices were analyzed using a custom Python code (32), which identified brain regions where dopamine fluorescence changes exceeded twice the SD of baseline fluctuations upon stimulation. These dopamine "hotspots" were designated as regions of interest (ROIs), which we term dopamine release sites. Recent studies identified such release sites as tyrosine hydroxylase-positive axonal varicosities colocalized with the presynaptic protein Bassoon (33, 34). Thus, the number of release sites in our labeled slices may closely correspond to the number of single synaptic dopamine release sites. Because nIRCats exhibit high sensitivity and a low detection limit (35), they can effectively respond to dopamine release when it is at or above the sensor's nanomolar sensitivity (33).

The degree of fluorescence modulation in each release site was quantified as $\Delta F/F_0$, defined as the fluorescence change ($F\text{-}F_0$) divided by baseline fluorescence (F_0), where peak $\Delta F/F_0$ corresponds to the amount of dopamine released from each release site. Therefore, the total amount of released dopamine is a function of both the number of release sites and the peak $\Delta F/F_0$ in each release site, and we used these two parameters to characterize dopamine release. Multiple measurements were performed for each brain slice to calculate the slice-averaged number of release sites and peak $\Delta F/F_0$ (Fig. 1*B*).

We first imaged dopamine release prompted by a single-pulse electrical stimulation applied under two different stimulation strength conditions to induce varying levels of dopamine release by adjusting the stimulation current and the distance between the imaging field of view and the electrode (Fig. 1*C*). When a stimulation current greater than 0.3 mA was applied with the electrode positioned close (5 μm) to the field of view, the number of release sites became saturated and did not change with further increases in current beyond 0.3 mA (Fig. 1*D*). This strong stimulation condition enabled activation of the maximum number of dopamine release sites, without saturating the $\Delta F/F_0$ within individual sites (*SI Appendix*, Fig. S1) or depleting the readily releasable pool of dopamine. We referred to this condition as "MAX," as it represents the maximum observable dopamine release in a field of view upon stimulation and likely represents a supraphysiological level of dopamine release. In contrast, when the electrode was positioned 80 μm away from the imaging field of view, changes in stimulation current significantly affected the amount of dopamine release (Fig. 1*D*). [$\Delta F/F_0$: $P = 0.024$ (0.1 mA & 0.3 mA), $P = 0.011$ (0.1 mA & 0.3 mA), $P = 0.037$ (0.3 mA & 0.5 mA) Release site: $P = 0.047$ (0.1 mA & 0.3 mA), $P = 0.026$ (0.1 mA & 0.3 mA, $P = 0.297$ (0.3 mA & 0.5 mA)]. The enhancement of dopamine release reflected both the activation of additional release sites and elevated $\Delta F/F_0$ within individual sites, with the latter contributing more substantially. In this "non-MAX" condition, only a portion of vesicles are released from the readily releasable dopamine pool (Fig. 1*C*). We chose 0.3 mA with the stimulator placed 80 μm away from the field of view as a representative non-MAX condition to investigate nonsaturated dopamine release.

We primarily focused on female meadow voles housed in short or long photoperiods, as females undergo a more pronounced transition in social behavior induced by season or photoperiod than males. We first assessed the effect of photoperiod alone, using matched housing across short and long photoperiods. Because social grouping and photoperiod normally shift in tandem for females (i.e., in the summer females live alone, but in winter they live in groups), we next assessed voles in "naturalistic housing" (alone in long photoperiods, or in a group of four in short photoperiods). Finally, since both females and males huddle in mixed sex groups during the winter, we also investigated the effect of sex in groups housed in short photoperiods for both MAX and Non-MAX conditions.

Max Stimulation Effects. We applied MAX stimulation to the dorsomedial striatum (DMS) of short photoperiod and long photoperiod voles. We chose to investigate the dorsal striatum due to its dense dopaminergic innervation and the absence of norepinephrine-releasing inputs, which the catecholamine sensors can also detect (36).

We first investigated the influence of daylength on dopamine release. In this cohort, voles in both long and short photoperiods were pair-housed, with only the photoperiod varied to precisely assess its effect on dopamine release under MAX stimulation protocols. MAX stimulation evoked an instantaneous increase in nIRCat fluorescence in both photoperiods. This fluorescence response was reversible, with fluorescence levels returning to baseline after 15 s through a combination of dopamine reuptake and diffusion away from the release site (Fig. 2 *A* and *B*). The peak $\Delta F/F_0$ was then calculated for each release site, rather than the entire field of view, to better quantify the relative amount of dopamine released as the release site density across experimental groups. As shown in Fig. 2*C*, pair-housed voles in short photoperiods had significantly larger peak $\Delta F/F_0$, indicating more dopamine release than pair-housed voles in long photoperiods ($P = 0.0036$, n = 8 voles in LP, 7 voles in SP). There was not a significant difference between the number of release sites in long and short photoperiods ($P = 0.26$, n = 8 voles in LP, 7 voles in SP).

Then, to assess whether the effect of photoperiod on dopamine release persisted in more naturalistic housing, we assessed voles in long, nonsocial photoperiods housed alone, and voles in short, social photoperiods housed in groups of four. These groups reflect the combined photoperiod and social environment change that female voles would experience in the wild and self-select in the lab. Social voles in short photoperiods (Social/SP) had a larger peak of $\Delta F/F_0$ than solitary voles in long photoperiods ($P = 0.05$, n = 7 voles in LP, 6 voles in SP) (Fig. 2*D*). Social/SP voles also had a higher number of release sites than solitary/long photoperiod voles ($P = 0.0068$, n = 7 voles in LP, 6 voles in SP) (Fig. 2*D*). Data from both studies were then compared. No significant effect of housing was detected within LP (pair versus or solo, ROI: $P = 0.80$; $\Delta F/F_0$: $P = 0.75$) or within SP (pair versus group, ROI: $P = 0.97$; $\Delta F/F_0$: $P = 0.16$). Data were thus pooled by day length for visualization (Fig. 2*A*) and subsequent analysis. In the pooled dataset, voles in short photoperiods had a significantly higher

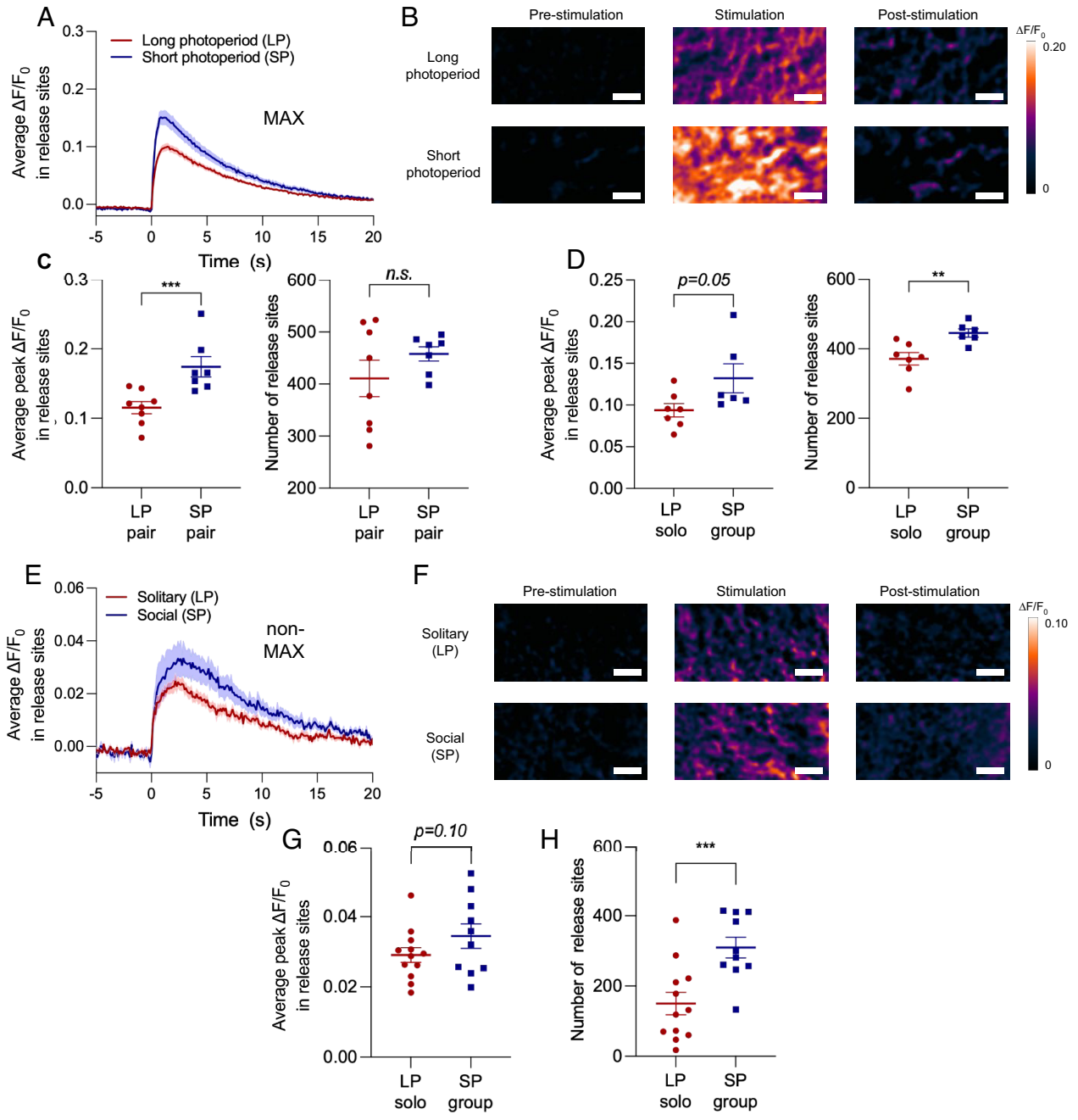

Fig. 2. Comparison of dopamine release dynamics in long photoperiods and short photoperiods. In slice, imaging electrically evoked dopamine in the DMS of voles housed in long photoperiods (LP, in red) and short photoperiods (SP, in blue) following a 0.5 mA electrical stimulation applied adjacent to the field of view (MAX, *A–D*) and a 0.3 mA electrical stimulation applied 80 μm away from the field of view (non-MAX, *E–G*). (*A*) Average $\Delta F/F_0$ in release sites time trace (solid line) with the SE (shadow). (*B*) $\Delta F/F_0$ response images within the same field of view, (*C*) average peak $\Delta F/F_0$ in each release site, and number of release sites in the MAX condition for pair-housed voles in both photoperiods. (n = 8 animals in LP, n = 7 animals in SP). (*D*) Average peak $\Delta F/F_0$ in each release site, and number of release sites in the MAX condition for solo-housed voles in LP and group housed voles in SP. (n = 7 animals in LP, n = 6 animals in SP). (*E*) Average $\Delta F/F_0$ in release sites time trace (solid line) with the SE (shadow). (*F*) $\Delta F/F_0$ response images within the same field of view, (*G*) average peak $\Delta F/F_0$ in each release site, and (*H*) number of release sites in the non-MAX condition. (n = 12 brain slices from 12 animals in long photoperiods housed alone, n = 11 brain slices from 11 animals in short photoperiods housed in groups) "Prestimulation," "Stimulation," and "Poststimulation" represent nanosensor fluorescence before, immediately following, and after electrical stimulation, respectively. (Scale bar: 10 μm.), n.s.: not significant, $*P < 0.05$, $**P < 0.01$, $***P < 0.005$.

$\Delta F/F_0$ ($P = 0.001$) and significantly more release sites ($P = 0.017$) than voles in long photoperiods. Social housing may act as a stressor for long photoperiod voles. Therefore, as changes in dopamine release were evident in both housing paradigms (matched housing across day lengths and naturalistic housing), we standardized on naturalistic housing to better emulate seasonal environmental changes for all future experiments.

Non-MAX Stimulation Effects. We next applied Non-MAX stimulation to the DMS of a new cohort of voles in both long and short photoperiods in naturalistic housing (alone in long photoperiods and in a group of four in short photoperiods). Non-MAX stimulation resulted in an increase in dopamine release in both short and long photoperiods, with much less dopamine release observed in both cohorts compared to the MAX stimulation

condition, as shown in Fig. 2 *E–G*. Under non-MAX stimulation conditions, nIRCats again showed clear reversibility, with their fluorescence returning to baseline as dopamine is reuptaken and diffuses away from the release site within 10 s of stimulation.

Under these non-MAX stimulation conditions, group-housed voles in short photoperiods showed a trend toward increased dopamine release per site compared to solitary long photoperiod voles, although the difference was not statistically significant ($P = 0.10$; n = 12 brain slices in LP, n = 10 brain slices in SP) (Fig. 2*G*). As for release sites, voles in short photoperiods showed a significantly larger number of release sites (310 ± 29, n = 10 brain slices) than those in long photoperiods (150 ± 31, n = 12 brain slices) ($P = 0.0008$) (Fig. 2*G*). Taken together, our data show that under mild stimulation conditions, group-housed voles in short, social photoperiods exhibited more activated dopamine release sites than solitary voles in long photoperiods, though release sites effluxed similar quantities of dopamine per site between photoperiods.

Finally, it is known that voles of both sexes housed in a short photoperiod form selective preferences for known (versus unknown) same-sex conspecifics and huddle in groups (9, 37). To identify whether sex differences in dopamine release exist, we assessed male and female meadow voles housed in groups of four in short photoperiods. Because of their similar social behavior in this photoperiod, we hypothesized that group-housed males and females would not show significant differences in dopamine release. Upon applying MAX and non-MAX electrical stimulation in the DMS, indeed neither $\Delta F/F_0$ nor the number of release sites differed significantly between male and female voles in short photoperiods (*SI Appendix*, Figs. S2 and S3).

Regional Variability within the Dorsal Striatum. Having observed differences in dopamine signaling as a function of stimulation strength, we next studied whether there were subregional differences in dopamine signaling within the dorsal striatum of group-housed voles in short photoperiods. The dorsal striatum can be divided into two regions-the dorsomedial striatum (DMS) and the dorsolateral striatum (DLS). While both subregions are implicated in motor control, they serve distinct behavioral functions. Dopamine in the DMS plays a critical role in goal-directed behaviors and behavioral flexibility, while dopamine in the DLS is responsible for habitual behaviors and navigation (38, 39). To this end, dopamine was electrically evoked in these two regions within the same brain slices under MAX condition. Under MAX stimulation, we found no significant difference in peak $\Delta F/F_0$ in release sites between the DMS and DLS. However, the DMS had significantly more release sites than the DLS. (*SI Appendix*, Fig. S4)

Effects of D2 Autoreceptor Manipulation. Having examined differences in dopamine release dynamics across sexes, housing conditions, photoperiods, and striatal subregions, we next investigated how dopamine D2 autoreceptor manipulation affects evoked dopamine release in short and long photoperiods. D2 autoreceptors play a crucial role in regulating dopamine signaling by suppressing dopamine release and synthesis when necessary, maintaining homeostasis in the brain's dopamine system. These receptors are primarily located on the presynaptic terminals of dopaminergic neurons (Fig. 1*C*). When dopamine is released into the synaptic cleft, it can bind to these autoreceptors, which then send a feedback signal to the neuron to reduce further dopamine release and synthesis. Due to their critical function, D2 autoreceptors have been widely studied in the context of dopamine-related psychiatric diseases such as Parkinson's disease and schizophrenia. (40–42).

It has previously been demonstrated that nIRCats are compatible with dopamine pharmacology, including the use of sulpiride (a D2 autoreceptor antagonist) and quinpirole (a D2 autoreceptor agonist) (12). Based on our above data showing differences in dopamine release site density and amount as a function of photoperiod, we hypothesized that solitary and social voles may have differing levels of dopamine receptor sensitivity to pharmacological intervention. We first examined the effects of sulpiride, a D2 autoreceptor antagonist, on electrically evoked dopamine release in voles housed alone in long photoperiods and in groups in short photoperiods. After imaging dopamine release in artificial cerebrospinal fluid (ACSF), 5 μM of sulpiride was bath-applied for 30 min and electrically evoked dopamine release was then imaged in the same field of view. For this experiment, non-MAX stimulation was used exclusively, as overstimulation could override any effects of the applied pharmacological agents.

We found that a 5 μM concentration of sulpiride significantly increased dopamine release in the DMS, as shown in Fig. 3 *A* and *B*. $\Delta F/F_0$ per release site in voles in long photoperiods increased by 74%, from a peak $\Delta F/F_0$ of 0.031 ± 0.002 presulpiride to 0.054 ± 0.006 postsulpiride (n = 5 brain slices), while in short photoperiods, the peak $\Delta F/F_0$ increased by 92%, from 0.037 ± 0.005 presulpiride to 0.072 ± 0.012 postsulpiride (n = 5 brain slices) (Fig. 3*C*). These results confirm that antagonism of presynaptic D2 autoreceptors using sulpiride effectively increases the amount of dopamine released from each dopamine release site.

While the application of 5 μM sulpiride increased the amount of dopamine released per release site in both photoperiods, sulpiride's effects were less evident in the number of release sites, which were not significantly different from pretreatment in either long or short photoperiods (Fig. 3*D*). Interestingly, after 5 μM sulpiride treatment, most release sites in short photoperiod voles were activated, with the number of release sites approaching that seen during MAX stimulation conditions (452 ± 9, n = 13 brain slices) (Fig. 2*D*). However, even with 5 μM sulpiride, most dopamine release sites in long photoperiod voles remained deactivated, and the number of release sites fell short compared to those measured with MAX stimulation conditions (392 ± 20, n = 15 brain slices).

Next, we investigated how quinpirole, a D2 autoreceptor agonist, affects electrically evoked dopamine release in the DMS of solitary voles in long photoperiods and group-housed voles in short photoperiods. Dopamine release upon non-MAX electrical stimulation was measured in the same field of view before and after bath application of 5 μM quinpirole. Surprisingly, although quinpirole substantially reduced integrated fluorescence across the field of view, the amount of dopamine released from each release site decreased only marginally in voles in long and short photoperiods (Fig. 3 *E–G*). The $\Delta F/F_0$ measured from release sites changed from 0.028 ± 0.004 and 0.036 ± 0.007 prequinpirole to 0.024 ± 0.004 and 0.026 ± 0.002 postquinpirole for long (n = 7 brain slices) and short (n = 6 brain slices) photoperiods, respectively. Instead, the major source of the clear decrease in dopamine response was the reduction in the number of dopamine release sites. The number of release sites decreased in short photoperiod voles by 55%, from 307 ± 48 prequinpirole to 137 ± 49 postquinpirole (n = 6 brain slices), while the release site number in long photoperiod voles was reduced by 88%, from 165 ± 50 prequinpirole to 20 ± 5 postquinpirole (n = 7 brain slices). Although voles in short photoperiods retained nearly half of their release sites after quinpirole application, dopamine release sites in long photoperiod voles were mostly deactivated, suggesting that these solitary voles in long photoperiods may have a higher sensitivity to D2 autoreceptor agonism relative to their social counterparts in short photoperiods. This could potentially be due to

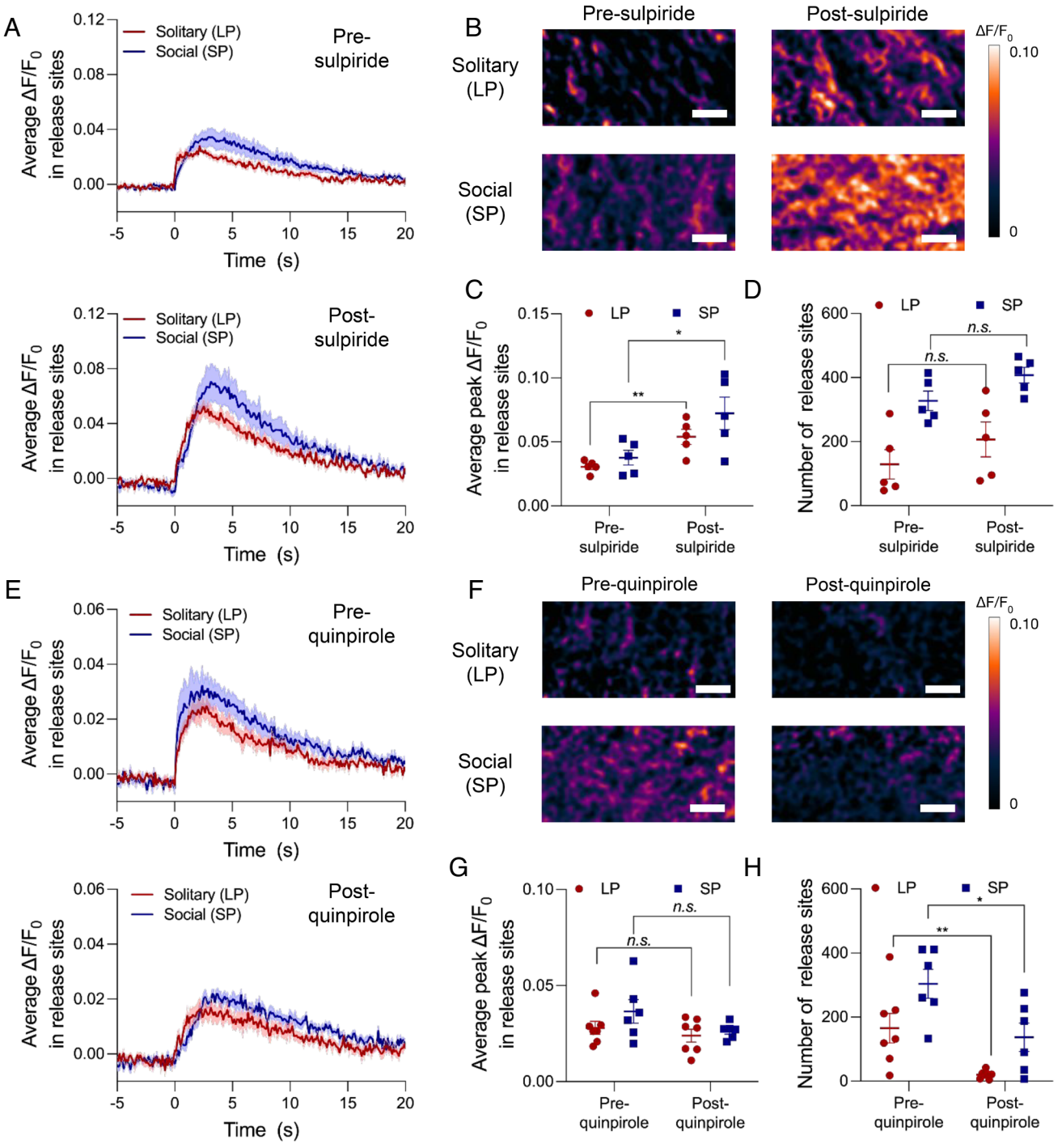

Fig. 3. Effects of D2 autoreceptor manipulation. In slice, effects of D2-autoreceptor antagonist (sulpiride, *A–D*) and agonist (quinpirole, *E–H*) on electrically evoked dopamine release of voles housed alone in long photoperiods (LP; in red); and housed in groups in short photoperiods (SP; in blue). (*A*) Average $\Delta F/F_0$ in each release site's time trace (solid line) with the SE (shadow), (*B*) $\Delta F/F_0$ response images, (*C*) average peak $\Delta F/F_0$, and (*D*) number of release site following a 0.3 mA single-pulse electrical stimulation in the DMS of voles in solitary and social conditions before and after 5 μM sulpiride treatment. (n = 5 brain slices from 5 animals for LP voles, n = 5 brain slices from five animals for SP voles) (*E*) Average $\Delta F/F_0$ in each release site's time trace (solid line) with the SE (shadow), (*F*) $\Delta F/F_0$ response images, (*G*) average peak $\Delta F/F_0$ and (*H*) number of release sites following a 0.3 mA single-pulse electrical stimulation in the DMS of voles in social and solitary conditions before and after 5 μM quinpirole treatment. (n = 7 brain slices from seven animals for solitary LP voles, n = 6 brain slices from six animals for social SP voles) (Scale bar: 10 μm.), n.s.: not significant, $*P < 0.05$, $**P < 0.01$, $***P < 0.005$.

altered D2 autoreceptor expression or autoreceptor functional responsiveness. We did not see a statistically significant difference between photoperiods in D2 receptor mRNA expression (*SI Appendix*, Fig. S5), although this pilot dataset of n = 4 animals is insufficient to conclude whether differences in pharmacological sensitivities are due to changes in autoreceptor expression or downstream differences in sensitivity.

Based on our measurements, we identified several characteristics of how D2 autoreceptors are differentially manipulated by dopamine receptor pharmacology within and between photoperiods. Although both drugs affect the number of dopamine release sites and the amount of dopamine released from each site to some extent, they operate through different mechanisms. Specifically, sulpiride is more effective at increasing the amount of dopamine

released from each site, while quinpirole is better at deactivating release sites in both photoperiod-housing conditions. In addition, we found that voles in short, social photoperiods respond more sensitively to sulpiride, which increases dopamine, but are less responsive to quinpirole, which decreases dopamine.

Extracellular Ca^{2+} Effects. Finally, we investigated how extracellular Ca^{2+} affects electrically evoked dopamine release in naturalistically housed voles in long and short photoperiods. The release of neurotransmitters such as dopamine from presynaptic dopaminergic neurons is highly dependent on the influx of Ca^{2+} through voltage-gated calcium channels (Fig. 1*C*). Consequently, the amount of dopamine released is influenced by the concentration of extracellular Ca^{2+}. We hypothesized that voles in long, nonsocial photoperiods, and short, social photoperiods might differentially respond to varying concentrations of extracellular Ca^{2+}, as suggested by our prior data showing differing sensitivities of each photoperiod to MAX versus non-MAX stimulation conditions.

For this experiment, acute brain slices from voles housed alone in long photoperiods, and in groups in short photoperiods, were prepared and incubated in Ca^{2+}-deficient ACSF buffer before imaging. This environment ensures that prior Ca^{2+} exposure does not influence dopamine release upon stimulation. Electrically evoked dopamine was imaged under non-MAX stimulation conditions in the Ca^{2+}-deficient buffer. After this initial imaging, Ca^{2+} was added to final concentrations of 2 mM and 5 mM, and dopamine release was imaged in the same field of view. In 0 mM Ca^{2+} buffer, we observed that dopamine release was highly suppressed in both conditions, as expected (Fig. 4). Solitary voles in long photoperiods exhibited a negligible amount of dopamine release, with a peak $\Delta F/F_0$ of 0.009 ± 0.004 and an average of 8 ± 3 release sites (n = 6 brain slices). Compared to dopamine release in regular ACSF buffer (Fig. 2 *E–H*), most dopamine release sites were deactivated (a 94% reduction in the number of release sites) in the absence of Ca^{2+}, and the few active sites released significantly smaller amounts of dopamine relative to standard 2 mM Ca^{2+} buffer conditions in long photoperiods. Interestingly, voles in short photoperiods still maintained some of their release sites even in a Ca^{2+}-deficient environment, with a peak $\Delta F/F_0$ of 0.016 ± 0.007 and an average of 68 ± 30 release sites (n = 5 brain slices). These observations suggest that social voles in short photoperiods exhibit higher resistance to Ca^{2+} deficiency in maintaining dopamine release, even in the absence of extracellular Ca^{2+}.

Next, a 2 mM Ca^{2+} buffer was supplied for 30 min, and upon stimulation, dopamine release became clearly observable, confirming that extracellular Ca^{2+} plays a critical role in dopamine release, as expected (Fig. 4*B*). Under these 2 mM Ca^{2+} extracellular calcium conditions, voles in short photoperiods exhibited both a higher peak $\Delta F/F_0$ (0.029 ± 0.003 for short photoperiods, n = 5 brain slices, and 0.022 ± 0.002 for long photoperiods, n = 6 brain slices) and a greater number of release sites compared to long photoperiod voles (231 ± 36 for short photoperiods, n = 5 brain slices, and 124 ± 27 for long photoperiods, n = 6 brain slices) (Fig. 4 *C* and *D*). It should be noted that when imaging was performed in regular ACSF without prior exposure to a 0 mM Ca^{2+} environment, the difference in peak $\Delta F/F_0$ between long and short photoperiods was insignificant (Fig. 2 *G* and *H*). These results indicate that voles in short, social photoperiod recover more quickly from Ca^{2+}-deficient conditions than their counterparts in long photoperiods. However, neither photoperiod showed full recovery of dopamine release to the levels observed when measured without prior exposure to a 0 mM Ca^{2+} environment. Next, a 5 mM Ca^{2+} buffer was supplied for another 30 min, which further increased both the peak $\Delta F/F_0$ and the number of release sites upon electrical stimulation. Short photoperiod voles exhibited a peak $\Delta F/F_0$ of 0.056 ± 0.006 and 429 ± 22 release sites (n = 5 brain slices). Interestingly, 5 mM of extracellular Ca^{2+} fully activated available dopamine release sites, whereby the observed number of release sites was comparable to that measured under MAX stimulation conditions (Fig. 2*D*). Although at 5 mM Ca^{2+} voles in long photoperiods also exhibited increases in peak $\Delta F/F_0$ (0.036 ± 0.005) and the number of release sites (222 ± 48, n = 6 brain

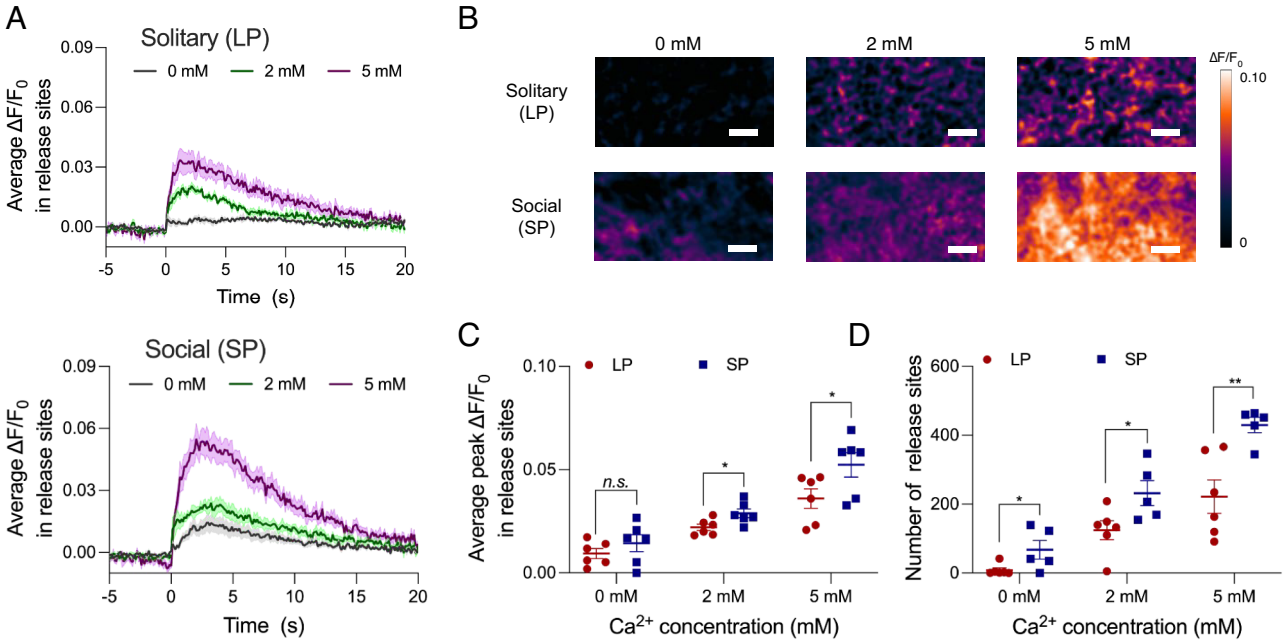

Fig. 4. Effects of extracellular Ca^{2+} on electrically evoked dopamine release of solitary voles in long photoperiods (LP; in red) and social voles in short photoperiods (SP, in blue). (*A*) Average $\Delta F/F_0$ in each release site's time trace (solid line) with the SE (shadow), (*B*) $\Delta F/F_0$ response images, (*C*) average peak $\Delta F/F_0$ and (*D*) number of release sites following a 0.3 mA single-pulse electrical stimulation in the DMS of voles in long and short photoperiods with various concentrations of Ca^{2+}. (n = 6 brain slices from six animals for solitary LP voles, n = 5 brain slices from five animals in social SP voles) (Scale bar: 10 μm.), n.s.: not significant, **P* < 0.05, ***P* < 0.01.

slices) relative to lower Ca^{2+} conditions, the release site numbers remained well below values observed under MAX stimulation (Fig. 2*D*).

In summary, based on all observations from varying extracellular Ca^{2+} concentrations, we confirmed that Ca^{2+} plays a significant role in gating dopamine release, with increasing Ca^{2+} levels leading to higher peak $\Delta F/F_0$ and a greater number of release sites. Our findings are consistent with previous studies showing that elevated extracellular calcium concentrations can increase the likelihood of neurotransmitter vesicle release, expand the size of the readily releasable pool, and shift inactive boutons into more active states (43, 44). Similar to what we observed with D2 autoreceptor drugs, voles housed in short, social photoperiods showed lower dopamine suppression under zero Ca^{2+} concentrations, which reduces dopamine release, and demonstrated faster enhancement in dopamine release as Ca^{2+} concentrations increased.

This pattern, together with their higher release site density, indicates that photoperiod may affect both the availability of release machinery and its functional coupling with presynaptic Ca^{2+} channels across different Ca^{2+} conditions. As a result, dopamine signaling that remains stable at low Ca^{2+} levels while being strongly amplified at high Ca^{2+} levels may allow voles in short photoperiods to maintain reliable baseline transmission and produce robust surges of dopamine during heightened activity. This broader dynamic range may enable their dopaminergic system to flexibly scale with the demands of social interactions, providing a physiological basis for greater adaptability and plasticity in social behavior. In contrast, voles in long, nonsocial photoperiods display a smaller number of release sites which may translate to a narrower Ca^{2+}-dependent range of dopamine release, leading to more constrained dopaminergic signaling and reduced capacity for modulation of social motivation and reward processing.

Discussion

Nontraditional species enable the study of multiple behaviors not found in model organisms. For example, meadow voles undergo a transition in social behavior in response to photoperiod that allows us to examine how changes in the brain contribute to changes in social behavior (and vice-versa). Studying nonmodel organisms comes with trade-offs, however, many of the tools available in model organisms are genetically based and may not work across nonmodel species. In this study, we use nIRCats to explore dopamine dynamics in meadow voles, between photoperiods linked to group size. We observed striking differences in synaptic-scale striatal dopamine signaling between voles housed in long and short photoperiods, both in matched and naturalistic (photoperiod-typical) group sizes.

Across a wide variety of experimental conditions including stimulation profiles, Ca^{2+} concentrations, agonist and antagonist applications, evoked dopamine was altered in a consistent manner. Photoperiod alone significantly influenced the amount of dopamine released per site with a nonsignificant trend toward increased release sites, while voles in naturalistic housing (alone in LP and social in SP) had significant effects on dopamine release per site and number of release sites. There were no detectable housing differences and pooled analysis revealed a greater number of dopamine release sites and higher dopamine release per site in voles housed in short photoperiods in the MAX condition. Having explicitly tested effects of both photoperiod alone, and photoperiod in the context of naturalistic housing (with solitary long photoperiod voles housed alone, and social short period voles housed in groups), all further experiments were conducted using naturalistic housing. Under mild (non-MAX) stimulation, voles in short photoperiods again activated more release sites than those in long photoperiods, but there was no difference in the amount of dopamine each site released. Additionally, we observed that voles in short photoperiods demonstrated heightened resistance to conditions that reduce dopamine release, such as quinpirole treatment or lack of extracellular calcium. In the wild, winter groups are essential for survival and thermoregulation for meadow voles (15, 45, 46). It is possible that group living may be supported not only by elevated dopamine but also resistance to reduced dopamine, ensuring voles remain in a group throughout the winter. To the same end, voles in short photoperiods showed greater sensitivity to agents that increase dopamine release, such as sulpiride and 5 mM extracellular calcium, further supporting the role of dopamine in regulating social behaviors and the possibility of dopamine synthesis upregulation or differences in autoreceptor sensitivity induced by photoperiod.

While social behavior changes markedly across photoperiods, this change is part of a larger suite of physiological and behavioral traits that shift as animals prepare for the transition to a winter environment. In winter and short photoperiods, voles are reproductively quiescent, weigh less, decrease food intake (47), and are more active than those housed in long photoperiods (20). Increased dopamine levels in short, winter-like photoperiods may support this increase in locomotion and may also contribute to changes in motivational states related to reproduction, feeding, and other behavioral drives.

Interestingly, many rodent studies of the interactions between dopamine and photoperiod find evidence of *lower* dopamine in short photoperiods relative to long photoperiods (29–31), opposite the findings in this study. Humans, however, show increased striatal dopamine during the fall and winter (48), in line with findings in the present study, and there is some evidence in rodents that photoperiodic effects on dopamine vary between species and brain regions (31), further highlighting species-specific variation. Furthermore, social contexts can also impact dopamine. Historically, studies of social isolation on dopamine have shown an association between isolation and increased dopamine response (49–51). In meadow voles, isolation is not a stressor for voles in long, nonsocial photoperiods as it is in many other rodent species (52, 53), whereas paired housing may act as a stressor in long, but not short photoperiods. We tested voles in both matched and naturalistic housing conditions and found no differences by housing.

The nIRCats used in this study were used in slice preparation, which is most suitable for detecting stable alterations in release-site scale dopamine signaling, e.g., across different environmental conditions such as photoperiod. Our results compare differences in the number of release sites, and the amount of dopamine released per release site, where some conditions induce changes in one but not both metrics. These results highlight the importance of release site scale dopamine imaging to measure nuanced differences likely unobservable using bulk measurement approaches. As we look toward the future of nongenomically encoded sensor use, future studies will benefit from nIRCats or other sensors that are capable of imaging nonmodel organisms in vivo to measure context-dependent dopamine signaling. Additionally, since dopamine can act as a neuromodulator and alter the activity of other neuropeptides like oxytocin and cortisol that are known to vary seasonally, sensors that can measure multiple molecules simultaneously would be beneficial to further elucidate these relationships.

The present findings not only validate the use of nIRCats in voles but also highlight the importance of dopamine in modulating changes in social behavior due to photoperiod in meadow

voles. This work paves the way for future studies of dopamine signaling in nontraditional organisms and demonstrates the potential of nIRCats for advancing our understanding of neurotransmitter dynamics across species.

Materials and Methods

Animal Subjects. Meadow voles were bred locally at UC Berkeley in long photoperiods (14 h light: 10 h dark). Within 1 wk of weaning, voles were separated into experimental housing and either remained in long photoperiods or were moved to short photoperiods (10 h light: 14 h dark). For the initial experiments using the MAX stimulation protocols, female meadow voles were housed in one of four groups: housed alone in long photoperiods, housed in a pair in long photoperiods, housed in a pair in short photoperiods, or housed in a group of four in short photoperiods. When housed socially, cagemates were same-sex, age-matched conspecifics. For all other conditions, male and female meadow voles were housed in same-sex, age-matched groups of four in short photoperiods, and females were housed alone in long photoperiods. Voles were all adults at the time of the experiment. All animal procedures were approved by the University of California Berkeley Animal Care and Use Committee.

Materials. HiPco SWNTs were purchased from NanoIntegris (batch #27 to 104, diameter: 0.8 to 1.2 nm, length: 400 to 700 nm). $(GT)_6$ oligonucleotides purified with standard desalting were purchased from Integrated DNA Technologies. Quinpirole and sulpiride were purchased from Tocris Bioscience. All other agents were purchased from Millipore Sigma.

Sensor Synthesis and In Vitro Characterization. Near-infrared catecholamine sensors were synthesized using previously reported protocols. Briefly, SWNTs and $(GT)_6$ (2 mg each) were bath-sonicated (Branson Ultrasonic 1800) for 3 min in 1 mL of 0.1 M NaCl, followed by probe tip-sonication for 10 min (Cole-Parmer Ultrasonic Processor, 3-mm diameter tip, 5 W power) in an ice bath. To remove nondispered SWNTs, the resulting suspension was centrifuged at 16,000 g for 60 min (Eppendorf 5418), and the supernatant containing stable $(GT)_6$-SWNT was collected and used. The absorbance of the $(GT)_6$-SWNT was measured at 632 nm (NanoDrop One, Thermo Scientific) to calculate the SWNT concentration of the suspension. [extinction coefficient $\varepsilon = 0.036$ $(mg/L)^{-1}$ cm^{-1}] The $(GT)_6$-SWNT suspension was diluted to 5 $\mu g\ mL^{-1}$ and 200 $\mu g\ mL^{-1}$ for in vitro characterization and ex vivo slice experiments, respectively.

For in vitro characterization, fluorescence measurements were performed using a 20× objective on an inverted Zeiss microscope (Axio Observer D1) with a SCT 320 spectrometer (Princeton Instruments) and a liquid nitrogen-cooled InGaAs linear array detector (PyLoN-IR, Princeton Instruments). Aliquots of 99 μL of $(GT)_6$-SWNT were placed in each well of a 384-well plate. The fluorescence spectra of $(GT)_6$-SWNT were obtained before and after the addition of 1 μL of dopamine using a custom-built spectrometer and microscope. A 721 nm laser (Opto Engine LLC) was used to excite the nanosensor suspensions. nIRCats exhibit a 24-fold increase in fluorescence upon exposure to dopamine, with high selectivity against various neurochemicals in vitro (35).

Brain Slice Preparation and Sensor Labeling. Brain slices were prepared using established protocols (12, 13, 54). Briefly, meadow voles were anesthetized under isoflurane and then intraperitoneally injected with a combination of ketamine (10 mg mL^{-1}) and xylazine (5 mg mL^{-1}) in saline (1 mL). While anesthetized, transcardial perfusion was performed with ice-cold cutting buffer (119 mM NaCl, 26.2 mM $NaHCO_3$, 2.5 mM KCl, 1 mM NaH_2PO_4, 3.5 mM $MgCl_2$, 10 mM glucose, and 0 mM $CaCl_2$), followed by rapid brain dissection over the same buffer. The brain was mounted onto a vibratome (Leica VT 1000S) and coronally sliced into 300-μm-thick sections. Sections containing the dorsal striatum were incubated for 30 min at room temperature in oxygen-saturated ACSF buffer (119 mM NaCl, 26.2 mM $NaHCO_3$, 2.5 mM KCl, 1 mM NaH_2PO_4, 1.3 mM $MgCl_2$, 10 mM glucose, 2 mM $CaCl_2$). The slices were transferred to a small volume incubation chamber (Scientific Systems Design Inc., AutoMate Scientific) containing 5 mL of oxygen-saturated ACSF. nIRCat nanosensors were added to the incubation chamber (final concentration of 200 $\mu g\ mL^{-1}$), and slices were incubated for 15 min. Then, the slices were rinsed with ACSF buffer to remove excess nonlocalized sensors.

Dopamine Imaging in Acute Brain Slices. Slice imaging was performed using established protocols and a custom-built upright epifluorescent microscope (Olympus, Sutter Instruments) mounted onto a motorized stage (12, 13). A 785 nm laser (Opto Engine LLC) was used to excite nanosensors, which was expanded to a final diameter of ~1 cm using a Keplerian beam expander with two plano-convex lenses (f = 25 and 75 mm; AR coating B, Thorlabs) The beam was passed through a fluorescence filter cube [excitation: 800 nm shortpass (FESH0800), dichroic: 900 longpass (DMLP990R), and emission: 900 longpass (FELH0900); Thorlabs] to a 60× Apo objective (numerical aperture, 1.0; working distance, 2.8 mm; water dipping; high nIR transmission; Nikon CFI Apo 60XW nIR). Emission photons collected from the sample were passed through the filter cube, were focused onto a two-dimensional InGaAs array detector [500 to 600 nm: 40% quantum efficiency (QE); 1,000 to 1,500 nm: >85% QE; Ninox 640, Raptor Photonics] and were recorded using the Micro-Manager Open Source Microscopy Software.

A bipolar stimulation electrode (Platinum/Iridium Standard Tip, MicroProbes for Life Science) was positioned in the dorsal striatum using a 4× objective lens. A total of 600 frames were captured in the nIR using a 60× objective lens at eight frames per second, with electrical stimulation applied after 200 frames of baseline. For the saturated condition, the electrode was placed directly next to the field of view, and a single-pulse 0.5 mA stimulation was applied for 1 ms. For the nonsaturated condition, the electrode was placed 80 μm away from the field of view, and a single-pulse 0.3 mA stimulation was applied for 1 ms. nIRCats demonstrated fluorescence modulation in response to evoked dopamine release with high spatial (μm) and temporal (ms) resolution.

For drug experiments, imaging was initially conducted in plain ACSF. Then, either quinpirole or sulpiride (5 μM) was added to the imaging chamber through ACSF perfusion. The brain slice was incubated with either drug for 30 min before imaging continued in the same field of view. For calcium experiments, initial incubation occurred in ACSF without calcium, then calcium was later applied in concentrations of 2 mM and 5 mM. Brain slices were exposed to new calcium concentrations for 30 min before imaging.

Image Processing and Data Analysis. Image files were processed using a custom Python application (https://github.com/NicholasOuassil/NanoImgPro). A field of view was divided into 25 × 25 pixel grids, and those with fluorescence modulation more than two times the SD of baseline fluctuations were identified as ROIs, which we term release sites. Recent studies identified such release sites as tyrosine hydroxylase-positive axonal varicosities colocalized with the presynaptic protein Bassoon (33, 34). Thus, the number of release sites may closely correspond to the number of single synaptic dopamine release sites. $\Delta F/F_0$ of each release site was calculated as $(F-F_0)/F_0$, where F_0 is the average intensity of baseline fluorescence and F is the dynamic fluorescence intensity. $\Delta F/F_0$ was averaged over release sites to draw an average $\Delta F/F_0$ in release sites as a function of time. The maximum $\Delta F/F_0$ of each release site was identified and averaged to calculate the average peak $\Delta F/F_0$ in release sites. The total amount of released dopamine is a function of both the number of release sites and the peak $\Delta F/F_0$ in each release site, and we use these two parameters to describe electrically evoked dopamine release.

RT-qPCR. Six punches (2 mm in diameter) were collected from dorsomedial striatum per each animal, which were treated as one sample. RNA was extracted from pooled punches using the TRI reagent method following the manufacturer's instructions. To remove any contaminating DNA from samples, samples were treated with the TURBO DNA-free Kit from Invitrogen following the "rigorous" DNAse protocol. RNA was then converted to cDNA using the iScript cDNA synthesis kit (Bio-rad). RT-qPCR was run for each target in triplicate using 5 ng of cDNA per well and SYBR Green Universal master mix (Applied Biosystems). Primers for each target are listed below (Table 1). Primers for each target gene were designed using the NCBI primer design tool, and primers for the housekeeping gene, hypoxanthine-guanine phosphoribosyltransferase (HPRT), were taken from ref. 55 after confirming complementation with the *M. pennsylvanicus* genome. Melt curves were used to confirm amplification of only a single product per target. To control for DNA contamination, a no reverse transcriptase control (NRTC) was run for each sample–no amplification was observed in any of these samples, indicating successful DNA removal. For analysis, dCq values for each target were

Table 1. Primers used for qPCR

Target	Forward primer	Reverse primer
HPRT	CCC AGC GTC GTG ATT AGT GA	TCG AGC CAG TCT TTC AGT CC
DRD1	AGA AAC AAA TCC GGC GCA TC	TTC CAC GGG GTT GCC ATT AC
DRD2	CAA GCC AGA GAA GAA TGG GC	TAA GGG AGG TCC GGG TTT TG

calculated by taking the difference between the raw cycle count (Cq) of the target and Cq of the housekeeping gene. Fold change was calculated as 2^(−dCq). ddCq analysis was not conducted as we sought to simply directly compare mRNA expression across 2 d lengths and there was no "untreated" control for further normalization.

Data, Materials, and Software Availability. A custom image processing Python application is available online (https://github.com/NicholasOuassil/NanoImgPro) (32). Other data are included in the article and/or *SI Appendix*.

ACKNOWLEDGMENTS. This material is based upon work supported by the NSF Graduate Research Fellowship Program under Grant No. DGE 2146752 (K.C.P.) and DGE 1656518 (S.A.T.). Any opinions, findings, and conclusions or recommendations expressed in this material are those of the author(s) and do not necessarily reflect the views of the NSF. We acknowledge the support of a NSF CAREER Award 2239635 (A.K.B.), a NIH grant R01MH132908 (A.K.B.), a Burroughs Wellcome Fund Career Award at the Scientific Interface (N.K. and M.P.L.), a Dreyfus Foundation Award (M.P.L.), the Philomathia Foundation (M.P.L.), an NSF CAREER Award 2046159 (M.P.L.), McKnight Foundation Award (M.P.L.), a Simons Foundation Award (M.P.L.), a Moore Foundation Award (M.P.L.), a Heising-Simons Fellowship (M.P.L.), a Brain Foundation Award (M.P.L.), a Polymaths award from Schmidt Sciences, LLC (M.P.L.), and Schmidt Science Fellows, in partnership with the Rhodes Trust (N.K.). M.P.L. is a Chan Zuckerberg Biohub investigator.

Author affiliations: [a]California Institute for Quantitative Biosciences, University of California, Berkeley, CA 94720; [b]Department of Integrative Biology, University of California, Berkeley, CA 94720; [c]Department of Bioengineering, University of Illinois Urbana-Champaign, Urbana, IL 61801; [d]Department of Plant and Microbial Biology, University of California, Berkeley, CA 94720; [e]Helen Wills Neuroscience Institute, University of California, Berkeley, CA 94720; [f]Department of Neuroscience, University of California, Berkeley, CA 94720; and [g]Department of Chemical and Biomolecular Engineering, University of California, Berkeley, CA 94720

Author contributions: J.M., K.C.P., A.K.B., and M.P.L. designed research; J.M., K.C.P., N.K., and S.A.T. performed research; J.M., K.C.P., A.K.B., and M.P.L. analyzed data; and J.M., K.C.P., A.K.B., and M.P.L. wrote the paper.

Competing interest statement: Author N.K. and Editor C.M. are at the same institution but have not collaborated directly.

1. H. A. Krebs, The August Krogh principle: "For many problems there is an animal on which it can be most conveniently studied". *J. Exp. Zool.* **194**, 221–226 (1975).
2. A. Krogh, The progress of physiology. *Science* **1979**, 200–204 (1929).
3. M. Taborsky *et al.*, Taxon matters: Promoting integrative studies of social behavior: NESCent Working Group on Integrative Models of Vertebrate Sociality: Evolution, mechanisms, and emergent properties. *Trends Neurosci.* **38**, 189–191 (2015).
4. M. M. Yartsev, The emperor's new wardrobe: Rebalancing diversity of animal models in neuroscience research. *Science* **1979**, 466–469 (2017).
5. B. Behav, M. E. Hale, Toward diversification of species models in neuroscience. *Brain Behav. Evol.* **93**, 166–168 (2019).
6. G. Laurent, On the value of model diversity in neuroscience. *Nat. Rev. Neurosci.* **21**, 395–396 (2020).
7. H. A. Hofmann *et al.*, An evolutionary framework for studying mechanisms of social behavior. *Trends Ecol. Evol.* **29**, 581–589 (2014).
8. S. M. Phelps, P. Campbell, D.-J. Zheng, A. G. Ophir, Beating the boojum: Comparative approaches to the neurobiology of social behavior. *Neuropharmacology* **58**, 17–28 (2010).
9. N. S. Lee, A. K. Beery, Neural circuits underlying rodent sociality: A comparative approach. *Curr. Top. Behav. Neurosci.* **43**, 211–238 (2019).
10. R. Báez-Mendoza, W. Schultz, The role of the striatum in social behavior. *Front. Neurosci.* **7**, 71890 (2013).
11. J. P. Bhanji, M. R. Delgado, The social brain and reward: Social information processing in the human striatum. *WIREs Cogn. Sci.* **5**, 61–73 (2014).
12. A. G. Beyene *et al.*, Imaging striatal dopamine release using a nongenetically encoded near infrared fluorescent catecholamine nanosensor. *Sci. Adv.* **5**, eaaw3108 (2019).
13. S. J. Yang, J. T. Del Bonis-O'Donnell, A. G. Beyene, M. P. Landry, Near-infrared catecholamine nanosensors for high spatiotemporal dopamine imaging. *Nat. Protoc.* **16**, 3026–3048 (2021).
14. A. K. Beery, Frank Beach award winner: Neuroendocrinology of group living. *Horm. Behav.* **107**, 67–75 (2019).
15. D. M. Madison, Space use and social structure in meadow voles. *Microtus pennsylvanicus*. *Behav. Ecol. Sociobiol.* **7**, 65–71 (1980).
16. A. B. Webster, R. J. Brooks, Social behavior of *Microtus pennsylvanicus* in relation to seasonal changes in demography. *J. Mammal.* **62**, 738–751 (1981).
17. B. J. Prendergast, R. J. Nelson, I. Zucker, "Mammalian seasonal rhythms" in *Hormones, Brain and Behavior*, D. W. Pfaff, A. P. Arnold, S. E. Fahrbach, A. M. Etgen, R. T. Rubin, Eds. (Elsevier, 2002), pp. 93–156.
18. M. J. Paul, I. Zucker, W. J. Schwartz, Tracking the seasons: The internal calendars of vertebrates. *Philos. Trans. R. Soc. Lond. B Biol. Sci.* **363**, 341–361 (2008).
19. A. K. Beery, T. J. Loo, I. Zucker, Day length and estradiol affect same-sex affiliative behavior in the female meadow vole. *Horm. Behav.* **54**, 153–159 (2008).
20. K. C. Power, N. S. Lee, K. Rendon-Torres, D. A. W. Soergel, A. K. Beery, A social switch: Daylength drives meadow vole group dynamics in automatically tracked habitats. *Anim. Behav.* **222**, 123084 (2025), 10.1016/J.ANBEHAV.2025.123084.
21. A. K. Beery, I. Zucker, Oxytocin and same-sex social behavior in female meadow voles. *Neuroscience* **169**, 665–673 (2010).
22. A. K. Beery, D. M. Vahaba, D. M. Grunberg, Corticotropin-releasing factor receptor densities vary with photoperiod and sociality. *Horm. Behav.* **66**, 779–786 (2014).
23. A. M. J. Anacker, J. D. Christensen, E. M. LaFlamme, D. M. Grunberg, A. K. Beery, Septal oxytocin administration impairs peer affiliation via V1a receptors in female meadow voles. *Psychoneuroendocrinology* **68**, 156–162 (2016).
24. Z. Wang *et al.*, Dopamine D2 receptor-mediated regulation of partner preferences in female prairie voles (*Microtus ochrogaster*): A mechanism for pair bonding? *Behav. Neurosci.* **113**, 602–611 (1999).
25. Y. Liu, Z. X. Wang, Nucleus accumbens oxytocin and dopamine interact to regulate pair bond formation in female prairie voles. *Neuroscience* **121**, 537–544 (2003).
26. S. L. Resendez *et al.*, Dopamine and opioid systems interact within the nucleus accumbens to maintain monogamous pair bonds. *Elife* **5**, e15325 (2016).
27. A. F. Pierce *et al.*, Nucleus accumbens dopamine release reflects the selective nature of pair bonds. *Curr. Biol.* **34**, 519–530.e5 (2024).
28. B. J. Aragona *et al.*, Nucleus accumbens dopamine differentially mediates the formation and maintenance of monogamous pair bonds. *Nat. Neurosci.* **9**, 133–139 (2006).
29. A. N. Jameson *et al.*, Photoperiod impacts nucleus accumbens dopamine dynamics. *ENeuro* **10**, ENEURO.0361-22.2023 (2023).
30. S. P. Deats, W. Adidharma, L. Yan, Hypothalamic dopaminergic neurons in an animal model of seasonal affective disorder. *Neurosci. Lett.* **602**, 17–21 (2015).
31. R. Goda *et al.*, Serotonin levels in the dorsal raphe nuclei of both chipmunks and mice are enhanced by long photoperiod, but brain dopamine level response to photoperiod is species-specific. *Neurosci. Lett.* **593**, 95–100 (2015).
32. N. Ouassil, Nanosensor image processor (NanoImgPro), a python-based image analysis tool for dopamine nanosensors. https://github.com/NicholasOuassil/NanoImgPro (Accessed 11 March 2025).
33. S. Elizarova *et al.*, A fluorescent nanosensor paint detects dopamine release at axonal varicosities with high spatiotemporal resolution. *Proc. Natl. Acad. Sci. U.S.A.* **119**, e2202842119 (2022).
34. C. Bulumulla *et al.*, Visualizing synaptic dopamine efflux with a 2D composite nanofilm. *Elife* **11**, e78773 (2022).
35. A. G. Beyene *et al.*, Ultralarge modulation of fluorescence by neuromodulators in carbon nanotubes functionalized with self-assembled oligonucleotide rings. *Nano Lett.* **18**, 6995–7003 (2018).
36. C. W. Berridge, B. D. Waterhouse, The locus coeruleus–noradrenergic system: Modulation of behavioral state and state-dependent cognitive processes. *Brain Res. Rev.* **42**, 33–84 (2003).
37. A. K. Beery, D. M. Routman, I. Zucker, Same-sex social behavior in meadow voles: Multiple and rapid formation of attachments. *Physiol. Behav.* **97**, 52–57 (2009).
38. Y. Vandaele *et al.*, Distinct recruitment of dorsomedial and dorsolateral striatum erodes with extended training. *Elife* **8**, e49536 (2019).
39. B. D. Devan, N. S. Hong, R. J. McDonald, Parallel associative processing in the dorsal striatum: Segregation of stimulus–response and cognitive control subregions. *Neurobiol. Learn. Mem.* **96**, 95–120 (2011).
40. C. P. Ford, The role of D2-autoreceptors in regulating dopamine neuron activity and transmission. *Neuroscience* **282**, 13–22 (2014).
41. P. Seeman, Schizophrenia and dopamine receptors. *Eur. Neuropsychopharmacol.* **23**, 999–1009 (2013).
42. K. Fuxe, D. Marcellino, S. Genedani, L. Agnati, Adenosine A2A receptors, dopamine D2 receptors and their interactions in Parkinson's disease. *Mov. Disord.* **22**, 1990–2017 (2007).
43. J. Leitz, E. T. Kavalali, Ca2+ influx slows single synaptic vesicle endocytosis. *J. Neurosci.* **31**, 16318–16326 (2011).
44. M. S. Thanawala, W. G. Regehr, Presynaptic calcium influx controls neurotransmitter release in part by regulating the effective size of the readily releasable pool. *J. Neurosci.* **33**, 4625–4633 (2013).
45. D. M. Madison, W. J. McShea, Seasonal changes in reproductive tolerance, spacing, and social organization in meadow voles: A microtine model. *Am. Zool.* **27**, 899–908 (1987).
46. N. R. Ondrasek *et al.*, Environmental modulation of same-sex affiliative behavior in female meadow voles (*Microtus pennsylvanicus*). *Physiol. Behav.* **140**, 118–126 (2015).
47. J. Dark, I. Zucker, G. N. Wade, Photoperiodic regulation of body mass, food intake, and reproduction in meadow voles. *Am. J. Physiol.* **245**, R334–R338 (1983).
48. D. P. Eisenberg *et al.*, Seasonal effects on human striatal presynaptic dopamine synthesis. *J. Neurosci.* **30**, 14691–14694 (2010).
49. F. S. Hall *et al.*, Isolation rearing in rats: Pre- and postsynaptic changes in striatal dopaminergic systems. *Pharmacol. Biochem. Behav.* **59**, 859–872 (1998).
50. J. T. Yorgason *et al.*, Social isolation rearing increases dopamine uptake and psychostimulant potency in the striatum. *Neuropharmacology* **101**, 471–479 (2016).
51. A. N. Karkhanis *et al.*, Chronic social isolation stress during peri-adolescence alters presynaptic dopamine terminal dynamics via augmentation in accumbal dopamine availability. *ACS Chem. Neurosci.* **10**, 2033–2044 (2019).

52. J. T. Curtis, J. R. Stowe, Z. Wang, Differential effects of intraspecific interactions on the striatal dopamine system in social and non-social voles. *Neuroscience* **118**, 1165–1173 (2003).
53. J. Stowe, Y. Liu, J. Curtis, M. Freeman, Z. Wang, Species differences in anxiety-related responses in male prairie and meadow voles: The effects of social isolation. *Physiol. Behav.* **86**, 369–378 (2005).
54. D. J. Piekarski, J. R. Boivin, L. Wilbrecht, Ovarian hormones organize the maturation of inhibitory neurotransmission in the frontal cortex at puberty onset in female mice. *Curr. Biol.* **27**, 1735–1745. e3 (2017).
55. E. M. Vitale *et al.*, Partner-seeking and limbic dopamine system are enhanced following social loss in male prairie voles (*Microtus ochrogaster*). *Genes Brain Behav.* **22**, e12861 (2023).